Hydrogen plasmas beyond density-functional theory: Dynamic correlations and the onset of localization

François Perrot
Centre d'Etudes de Limeil, Commissariat à l'Energie Atomique, Boîte Postale 27, F-94190 Villeneuve St. Georges, France

M. W. C. Dharma-wardana
Division of Physics, National Research Council of Canada, Ottawa K1A 0R6, Canada
(Received 5 October 1983)

We examine the onset of bound (i.e., localized) states in a high-temperature plasma consisting of electrons and ions. The onset of localization or ionization is related to the Mott and Anderson transitions of condensed-matter physics and to the breakdown of the Saha equation. We consider several models and develop a physically reasonable model of a plasma based on density-functional theory (DFT) where the mean ionic charge $\bar{Z}$ interpolates from the fully ionized limit to the atomic limit. This DFT model provides structure factors and Kohn-Sham eigenstates which are then used to calculate the self-energy of the one-electron Green function, thus transcending the local-density approximation and the well-known limitations of DFT, especially with regard to the excitation spectrum. The self-energy contains contributions from electron-electron and electron-ion density fluctuation effects, screening effects, and the renormalization of the propagators. The calculation yields shifted energy levels, widths, and level populations. The level widths are shown to be closely related to the electrical conductivity of Ziman-type formulations. The one-particle formalism used makes contact with the multiple-scattering theories of disordered materials, liquid metals, etc., and is a necessary first step to a future calculation of two-particle propagators and related properties.

I. INTRODUCTION

In a previous paper[1] (referred to as DP) we discussed how density-functional theory[2] (DFT) could be applied to the study of a system of ions and electrons in thermodynamic equilibrium at arbitrary temperatures and pressures. The method was illustrated by an application to hydrogen plasma over a range of physical situations where the strong coupling plasma parameter Γ varied from about 0.2 to 10 while the ion-sphere radius r_s^i varied from 1 to 2 a.u.; r_s^i and Γ are given by

$$r_s^i=\left[\frac{3}{4\pi\bar{\rho}}\right]^{1/3}, \quad \Gamma=\bar{Z}^2/(k_B T r_s^i) \tag{1.1}$$

where $k_B T=1/\beta$ is the thermal energy in atomic units and $\bar{\rho}$ is the mean density of the ions with an effective charge $\bar{Z}$. The plasma is ionized in the strongly coupled regime, but a weak $1s$-symmetry bound state begins to appear and deepens as the density is lowered and the temperature is increased. Then the ions can no longer be treated as having an effective charge $\bar{Z}=Z$, as was done in the numerical work presented in DP. A consistent theory of $\bar{Z}$ is needed for this purpose and in related contexts.[3]

The main objectives of this paper are (i) to set up a physically realistic model for estimating the mean ionic charge $\bar{Z}$, (ii) to set up a formal scheme which goes beyond DFT in that energy levels can be calculated with some confidence, and (iii) to use such a scheme for studying the onset and nature of localized states in a plasma as the density and temperature are varied.

The need for (ii) stems from the fact that the energy levels of DFT, obtained from the Kohn-Sham equation, cannot be rigorously identified with the one-particle states of the physical system. Further, the local density approximation (LDA) for the exchange-correlation potential[4] used in DFT calculations has to be transcended and the effects of dynamic correlations incorporated if the true levels, level widths, and level populations are to be determined. This is particularly important in the question of the onset of localization where the shallow $1s$ state is expected to be strongly influenced by the density fluctuations in the system. If the level width γ_{1s}, obtained from the self-energy Σ_{1s}, is small compared to the eigenvalue $|\epsilon_{1s}|$ we have a well-formed state. To simplify matters we shall confine the present study to a system having a single bound state.

The calculation of the energy levels which goes beyond DFT to approximate the true single-particle spectrum has to proceed via the Green-function technique. The Kohn-Sham eigenstates (DFT basis) will provide a representation for the one-particle Green function. Such a calculation is also a necessary step towards a future calculation of the two-particle Green function which determines the line spectrum (*line* shifts, widths) rather than the *level* spectrum of an atom in a plasma. Most of the necessary theory in the plasma context has already been discussed in Refs. 5 and 6.

The other interesting aspect of the onset of these localized states is its conceptual relation to the Mott[7] and Anderson transitions[7,8] which have been studied in the theory of solids, where the onset is posed in terms of the metal-

insulator transition. Localization is believed to involve the effects of screening (Mott), disorder (Anderson), or both. In a plasma there is certainly no long-range order (unless the ions are assumed to be frozen forming a lattice) and hence the statistical effects of the ion distribution as well as screening effects contribute to the onset of localized states. However, there is no "metal-insulator" transition (but there can be localization) for the conditions of temperature and pressure prevailing in a high-temperature plasma.

The weak 1s state obtained from the DFT calculation is not simply a bound state of the central ion alone, but is a bound state of the central ion *inclusive* of the ion distribution within the correlation sphere. Thus the weak localized electron is in an orbital spanning a cluster of ions when it emerges from the fully delocalized continuum. Then, as the localization increases, it becomes more and more concentrated into the region of a single ion-sphere volume around the central ion. At that stage the electron may be completely associated with the central ion, with practically no overlap with the field-ion distribution. Thus localization proceeds from the fully extended state to the fully atomic state via a weak bound state where the electron is effectively spread over a number of ionic centers in the correlation sphere.

The plan of the paper is as follows. In Sec. II we briefly review the DFT scheme and introduce a definition of the effective nuclear charge $\bar{Z}$ somewhat different from DP (in DP it was assumed that $\bar{Z}=Z$ in the calculations). This is used to calculate the onset of the localized state for a typical range of r_s and T, using DFT with the local density approximation as in DP. In Sec. III we discuss how the eigenstates of the Kohn-Sham equation could be used as a basis set (for second quantization, etc.) for a many-body perturbation calculation of the self-energy of the localized level, while at the same time correcting the limitations in the Kohn-Sham one-electron energies. The resulting expressions for the self-energy contain contributions from dynamic density fluctuations in the electron and ion systems. The summations over l quantum states which enter into the self-energy equations bring in the contributions from density fluctuations which break the spherical symmetry inherent in DFT which is a time-independent model. Most of the details of the simplified representations used for obtaining a computationally convenient form are relegated to the Appendix. Finally in Sec. IV we discuss the results for hydrogen plasma for a representative range of r_s and T using a jellium model, a fully-ionized-plasma model similar to that used in DP, a mean-ion-plasma model, and then the generalization inclusive of dynamic correlations.

II. THE DENSITY-FUNCTIONAL EQUATIONS

In this section we review the DFT equations used in DP for the convenience of the reader, and with specific attention to the question of extending their validity in obtaining the one-electron excitation spectrum. We consider a reference ion at the origin, and a large sphere of radius R around it, such that R is larger than the characteristic lengths (e.g., correlation lengths) of the system. Thus, for example, the ion-pair distribution function $g_{ii}(r)$ is essentially unity for $r \geq R$. This implies that the equilibrium one-particle distributions are those of a system with no long-range order. If the density distributions of electrons and ions around the central ion are denoted by $n(r)$ and $\rho(r)$, we have

$$n(r)=g_{ie}(r)\bar{n} \,, \tag{2.1}$$

$$\rho(r)=g_{ii}(r)\bar{\rho} \,, \tag{2.2}$$

and

$$\bar{n}=\bar{Z}\bar{\rho} \,, \tag{2.3}$$

where $\bar{n}$ and $\bar{\rho}$ are the mean-electron and -ion densities, while $\bar{Z}$ is the mean ionic charge which has to be determined self-consistently, as described later. Also, $g_{ie}(r)$ is the ion-electron pair distribution function such that $g_{ie}(r)\rightarrow 1$ for $r \geq R$.

Density-functional theory states that the equilibrium grand canonical potential $\Omega[n,\rho]$ is a unique functional of the density distributions n,ρ and is a minimum for the exact distributions. This variational property is shown to lead to an effective one-particle Schrödinger equation (Kohn-Sham equation) for the electrons, and another effective one-particle Gibbs-Boltzmann equation for the ions. The two equations have the form (see DP)

$$[-\tfrac{1}{2}\nabla^2+V_e^{\mathrm{KS}}(r)]\phi_\nu(r)=\epsilon_\nu\phi(r) \,, \tag{2.4}$$

$$\rho(r)=\bar{\rho}\exp^{[-V_i^{\mathrm{KS}}(r)/k_BT]} \,, \tag{2.5}$$

where V_e^{KS} and V_i^{KS} are effective one-particle Kohn-Sham potentials. These equations are to be solved self-consistently since $V_e^{\mathrm{KS}}(r)$ and $V_i^{\mathrm{KS}}(r)$ involve the electron and ion distributions.

The grand canonical potential is given as

$$\begin{aligned}
&\Omega[n,\rho]=T[n,\rho]+\Omega_e+\Omega_{ei}+\Omega_i \,,\\
&T[n,\rho]=\int F^0[n(\vec{r}),\rho(\vec{r})]d\vec{r} \,,\\
&\Omega_e=-\int\frac{Z}{r}n(\vec{r})d\vec{r}+\frac{1}{2}\int\frac{n(\vec{r})n(\vec{r}')}{|\vec{r}-\vec{r}'|}d\vec{r}\,d\vec{r}'+\int F_{\mathrm{xc}}^e[n]d\vec{r}-\mu_e\int n(\vec{r})d\vec{r} \,,\\
&\Omega_{ei}=-\int\frac{\bar{Z}n(r)\rho(r')}{|\vec{r}-\vec{r}'|}d\vec{r}\,d\vec{r}'+\int F_c^{ei}[n,\rho]d\vec{r} \,,\\
&\Omega_i=\bar{Z}\int\frac{Z}{r}\rho(r)d\vec{r}+\frac{\bar{Z}^2}{2}\int\frac{\rho(\vec{r})\rho(\vec{r}')}{|\vec{r}-\vec{r}'|}d\vec{r}\,d\vec{r}'+\int F_c^i[\rho]d\vec{r}-\mu_i\int\rho(r)d\vec{r} \,.
\end{aligned} \tag{2.6}$$

Here $T[n,\rho]$ is the kinetic energy functional of the *noninteracting* system, having the exact *interacting densities* n,ρ. μ_e and μ_i are electron and ion chemical potentials. The potential Ω_e contains an electron exchange-correlation term F^e_{xc}. This is evaluated in the local density approximation (LDA), using the exchange-correlation potential for a finite-temperature electron gas, evaluated using many-body theory,[4] so as to include the first-order exchange, "all-order" ring sum, and approximations to the other second-order graphs. We shall correct for the shortcomings of LDA using many-body perturbation theory in calculating the true energy levels of the system.

The ion grand canonical potential term Ω_i contains the ion-ion correlation contribution F^i_c. This is evaluated from the formalism of hypernetted chain (HNC) theory, while F^{ei}_c which appears in Ω_{ei} was considered to be negligible. The treatment of ion correlations using HNC theory is known to be very satisfactory for plasmas with Γ even up to ≈ 15 and hence no change will be made in this respect. However, the correlation effects arising from the ion-electron interaction are found to be important in regard to the onset of localized states.

In order to maintain electroneutrality, the actual functional minimized in DP is

$$\mathfrak{Q}[n,\rho]=\Omega[n,\rho]-\lambda\left[\bar{Z}\int\rho(r)dr-\int n(r)dr\right], \tag{2.7}$$

where λ is a Lagrange multiplier. Equations (2.4) and (2.5) result from equating the functional derivatives of $\mathfrak{Q}$ with respect to n and ρ, respectively, to zero. The effective potentials which go into Eqs. (2.4) and (2.5) appear as the functional derivatives:

$$V_e=\frac{\delta}{\delta n}(\Omega_e+\Omega_{ei}),\quad V_i=\frac{\delta}{\delta\rho}(\Omega_i+\Omega_{ei}). \tag{2.8}$$

They can be simplified to give the forms

$$\begin{aligned}V_e(r)&=-\left[\frac{Z}{r}+V_p(r)\right]+V^e_{xc}(r)+\phi_e(\bar{Z},r)-\mu_e,\\ V_i(r)&=\bar{Z}\left[\frac{Z}{r}+V_p(r)\right]+V^i_c(r)+\phi_i(\bar{Z},r)-\mu_i,\end{aligned} \tag{2.9}$$

where $V_p(r)$ is the Poisson potential due to the net charge distribution $\bar{Z}\rho(r)-n(r)$. The potentials $\phi_e(\bar{Z},r),\phi_i(\bar{Z},r)$ contain functional derivatives of the type $\delta\bar{Z}/\delta n$ and $\delta\bar{Z}/\delta\rho$. We shall discuss them later, in the context of a model for the definition of $\bar{Z}$. Defining the potential outside the correlations sphere ($r\geq R$) to be zero we can introduce the modified potentials and modified chemical potentials by

$$\begin{aligned}V^{KS}_e(r)&=V_e(r)-V_e(R),\\ V^{KS}_i(r)&=V_i(r)-V_i(R),\\ \bar{\mu}_e&=-\mu_e-V^e_{xc}(R)-\phi_e(\bar{Z},R)-\lambda,\\ \bar{\mu}_i&=\mu_i-V^i_c(R)-\phi_i(\bar{Z},R)+\bar{Z}\lambda.\end{aligned} \tag{2.10}$$

These potentials appear directly in the effective one-particle equations (2.4) and (2.5).

Nature of the localized state and the effective charge $\bar{Z}$

The Kohn-Sham equation, Eq. (2.4), has to be solved self-consistently, satisfying the requirements of the finite temperature Friedel sum rule,[9] etc., as discussed in DP. The set of Kohn-Sham eigenstates ϕ_ν are fully delocalized (denoted by ϕ_D) for high-Γ plasmas. However, as the density is decreased and the temperature increased, localized states $\phi_L=\phi_\nu$, $\nu=n,l,m$, with $\epsilon_\nu<0$ begin to appear. The electron distribution in such 1s-like states is shown in relation to the ion profile and the correlation sphere, in Fig. 1. The number of electrons localized in such a state is given by

$$n_L=2f_\nu=2/[1+\exp(\epsilon_\nu-\bar{\mu}_e)\beta] \tag{2.11}$$

and involves the modified chemical potential $\bar{\mu}_e$. A number of aspects of these localized levels are worthy of comment.

(i) The localized orbital is essentially a bound state of the inhomogeneous ion distribution inside the correlation sphere and not an atomic state of the central ion by itself, *unless* $|\phi_L|^2$ lies entirely in the central region where $g_{ii}(r)$ is negligible. The normalized electron-density profile is seen to be insensitive to changes in the ion-density profile (see Fig. 1).

(ii) The transition from a proper atomic state of the central ion ϕ_A to a fully delocalized state ϕ_D occurs through a continuous series of localized states ϕ_L, which extends over many ion centers. ϕ_L may also be thought of as representing an electron tunneling from one atomic center to another. These states are capable of supporting a hopping conductivity mode and are analogous to the localized states present in the band tails of disordered sys-

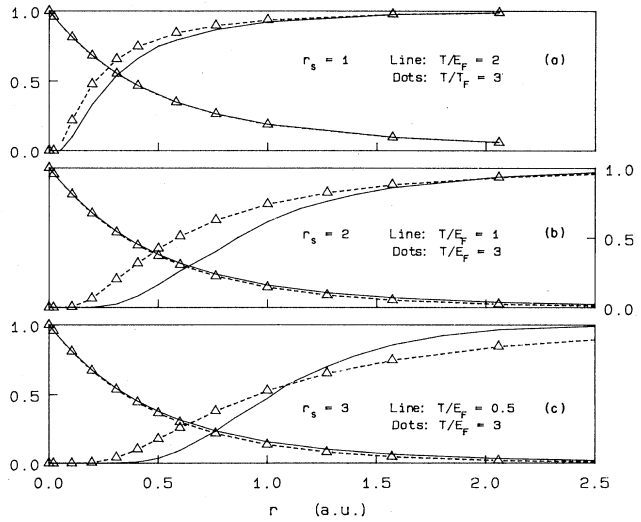

FIG. 1. The electron distribution $|\phi_{1s}(r)|^2$ of the weak 1s state normalized to unity at the origin is shown in relation to the ion distribution (normalized to unity at large r), for different values of r_s and T/E_F. See the caption to Table I for definitions of r_s and E_F.

tems and studied in the theory of the Mott-Anderson transition.

(iii) If the average number of bound electrons per ion is $\bar{n}_b$, then $\bar{Z}=Z-\bar{n}_b$. It is only in the atomic limit when $\phi_L \to \phi_A$ that we can set $\bar{n}_b = n_L$. In the intermediate case the definition of $\bar{n}_b$ involves some model for an "atom" in a plasma.[10] Since there is no real "boundary" between the "atom" and the plasma, it is really a convenient auxiliary concept allowing some possibilities of choice. The problem is equivalent to allocating an effective atomic radius $\bar{R}$ to each ion immersed in the plasma and arises in various guises in the statistical mechanics of plasmas. In the following we adopt a mean-ion-plasma (MIP) model such that the nuclear charge Z is fully compensated by the field charges contained inside the mean-ion radius $\bar{R}$. If $\bar{n}_f$ is the average free-electron density in the plasma and if n_f^i is the number of free electrons per ion, we have

$$n_f^i = \tfrac{4}{3}\pi \bar{R}^3 \bar{n}_f = (\bar{R}/r_s^e)^3 , \tag{2.12}$$

where r_s^e is the free-electron sphere radius. Then, if there is only a single localized state ϕ_{1s}, we define the number of bound electrons per ion to be

$$\bar{n}_b = 2\int_0^{\bar{R}} 4\pi r^2 \,|\,\phi_{1s}(r)\,|^2 f_{1s} dr , \tag{2.13}$$

where f_{1s} is the Fermi factor defined in (2.11). The effective ionic radius $\bar{R}$ is fixed by the condition

$$Z = \bar{n}_b + n_f^i . \tag{2.14}$$

Hence the effective ionic charge is given by

$$\bar{Z} = Z - \bar{n}_b . \tag{2.15}$$

These equations determine a mean ionic charge $\bar{Z}$ and a mean-ion radius $\bar{R}$ self-consistently, from the DFT equations. Typical results for $\bar{R}$ and $\bar{Z}$ in the MIP model are given in Table I. A convenient feature of this definition of $\bar{Z}$ and $\bar{R}$ is their relatively weak dependence on the distributions $n(r)$ and $\rho(r)$. It is also noteworthy that the potentials $\phi_i(\bar{Z},r), \phi_e(\bar{Z},r)$ drop out of the theory if the MIP definition of $\bar{Z}$ is adopted. Thus, since

$$\phi_i(r) = \int \left[\frac{Z}{r'} + V_p(r') - \lambda\right] \rho(r') \frac{\delta \bar{Z}[n(r),\rho(r)]}{\delta \rho(r)} dr' ,$$

$$\phi_e(r) = \int \left[\frac{Z}{r'} + V_p(r') - \lambda\right] \rho(r') \frac{\delta \bar{Z}[n(r),\rho(r)]}{\delta n(r)} dr' , \tag{2.16}$$

they become independent of r. Hence, since the potentials are normalized to zero outside the correlation sphere, they do not appear in the effective potentials used in the DFT equations.

III. EXTENSION BEYOND DENSITY-FUNCTIONAL THEORY

Although DFT is in principle exact in regard to the calculation of the pair distributions and other thermodynamic properties, it has three major limitations. These are (i) the use of a local density approximation for the exchange-correlation potentials, (ii) the lack of a formal basis for identifying the Kohn-Sham eigenfunctions and eigenvalues with suitable physical eigenstates of the system, and (iii) the lack of a technique, within DFT, for the calculation of lifetime effects.

TABLE I. The effective charge $\bar{Z}$ and the mean radius $\bar{R}$, in the mean-ion-plasma (MIP) model. $r_s = (3/4\pi\bar{n})^{1/3}$ a.u. Thus, for example, $r_s = 3$ corresponds to $\bar{n} \simeq 5.96 \times 10^{22}$ electrons/cm^3. $E_F = 1.8416/r_s$ a.u. $T/E_F = 1$ at $r_s = 3$ corresponds to 16.70 eV.

r_s	T/E_F	$\bar{R}$	$\bar{Z}$
1	2.0	0.9994	0.998
	2.5	0.9931	0.979
	3.0	0.9911	0.974
2	1.0	1.791	0.718
	1.5	1.799	0.728
	2.0	1.833	0.770
	3.0	1.887	0.840
	4.0	1.919	0.884
3	0.5	2.032	0.311
	1.0	2.130	0.358
	1.5	2.325	0.466
	2.0	2.490	0.572
	3.0	2.693	0.724
	4.0	2.797	0.810

In this context it should be noted that any method which uses, for example, Slater exchange and correlation or any other local density approximation, becomes immediately open to the first two limitations. Further, a theory of one-particle states which goes beyond the Hartree-Fock model must necessarily involve a quasiparticle description which involves finite lifetime effects. Such states are characterized by a Green function rather than by a wave function. Hence (ii) and (iii) are intimately connected with each other.

Some authors have attempted to go beyond the LDA using density-gradient expansions. Such methods are not easily justifiable and in any case do not lead to a proper theory of the excitation spectrum.

In order to transcend these limitations of DFT we need to use many-body theory. The DFT one-particle states ϕ_ν and eigenvalues ϵ_ν^0 can be used as a basis set for second quantization, retaining the accurate density profiles $\rho(r), n(r)$ already evaluated in DFT-LDA, as essential ingredients of the zeroth-order description. Within this approach we account for the density fluctuations $\delta\rho(r), \delta n(r)$, about the mean density profiles $\rho(r), n(r)$ by perturbation theory on the one-particle Green functions defined on the basis ϕ_ν.

We introduce Heisenberg operators $a_\nu, a_\nu^\dagger$ associated with the basis ϕ_ν and obeying Fermi commutation rules. The system Hamiltonian is

$$H = H^0 + H_I$$

with

$$H^0 = \sum_\nu \epsilon_\nu^0 a_\nu^\dagger a_\nu ,$$
$$H_I = \bar{V}_{ee} + \bar{V}_{ei} + \bar{V}_{ii} . \tag{3.1}$$

The bar over the symbols in this equation implies that the contributions in DFT corresponding to the Hartree-Fock field as well as the terms which were *already included* in the exchange-correlation potential V_{xc} are *excluded* in H_I.

The full ion-electron potential is

$$V_{ei}(r)=-\sum_{\alpha}\bar{Z}/|\vec{r}-\vec{R}_{\alpha}| =-\sum_{\vec{q}}\bar{Z}V_q e^{i\vec{q}\cdot\vec{r}}\rho_q \ , \tag{3.2}$$

where (setting the volume factor to unity) we have,

$$V_q=\frac{4\pi}{q^2}(1-\delta_{q,0}) \ ,$$

$$\rho_q=\sum_{\vec{k}} b^{\dagger}_{\vec{k}} b_{\vec{k}+\vec{q}}=\sum_{\alpha} e^{i\vec{q}\cdot\vec{R}_{\alpha}} \ .$$

Here ρ_q is the ion-density fluctuation and may be treated as a classical quantity, or as a quantum-mechanical operator using the operators $b_k, b_k^{\dagger}$, where $\vec{k}$ is an ion-momentum state. Hence (3.2) can be written in terms of the Fermi operators $a_\nu, a_\nu^{\dagger}$ as

$$V_{ei}=-\sum_{\vec{q},\nu_1,\nu_2}\bar{Z}V_q\langle\nu_1|e^{i\vec{q}\cdot\vec{r}}|\nu_2\rangle\rho_q a^{\dagger}_{\nu_1}a_{\nu_2}$$

$$=-\sum\langle 1|V_{ie}(q)|2\rangle\rho_q a^{\dagger}_1 a_2 \ . \tag{3.3}$$

This term describes the coupling of the ion-density fluctuation ρ_q with the electron-density fluctuation associated with the electronic transition $\nu_2\rightarrow\nu_1$.

The full electron-electron interaction is given by

$$V_{ee}=\tfrac{1}{2}\sum_{i,j}1/|\vec{r}_i-\vec{r}_j|$$

$$=\tfrac{1}{2}\sum_{\vec{q},\nu_i}V_q\langle\nu_1|e^{i\vec{q}\cdot\vec{r}_1}|\nu_4\rangle\langle\nu_2|e^{-i\vec{q}\cdot\vec{r}_2}|\nu_3\rangle a^{\dagger}_{\nu_1}a^{\dagger}_{\nu_2}a_{\nu_3}a_{\nu_4}$$

$$=\tfrac{1}{2}\sum_{\vec{q},\nu_i}\langle 12|V_{ee}(q)|34\rangle a^{\dagger}_1 a^{\dagger}_2 a_3 a_4 \ . \tag{3.4}$$

Equation (3.1) contains $\bar{V}_{ii}$ which arises from the ion-ion interaction term V_{ii}. Since this was treated using the HNC scheme it is not limited by a local density approximation, unlike in the case of the electron-electron interactions. Further, in most situations it is sufficient to consider $\bar{V}_{ii}$ as contributing to the static screening of the interaction lines in the diagrams (see below).

We need to pass from V_{ei} and V_{ee} (and similarly V_{ii}) to the forms $\bar{V}_{ei}, \bar{V}_{ee}$ which do not contain the contributions already included in DFT. The simplest procedure is to note that DFT contains (i) all the Hartree-type mean-field contributions, as well as exchange contributions contained in V_{xc}, and (ii) correlation contributions V_c which have been included in constructing V_{xc}. These are essentially the ring sum contributions. Hence we work with the full potentials V_{ei} and V_{ee}, but reject all Hartree-Fock-type diagrams [Figs. 2(a)—2(e)] because of (i). The correlation contribution V_c used in Kohn-Sham theory is small and real, since $V_c(r,n(r))$ is a real local potential. Thus it can be corrected for by subtracting $\langle\phi_\nu|V_c(r,n(r))|\phi_\nu\rangle$ from the energy shift, calculated from the self-energy and given by $\mathrm{Re}\Sigma_\nu(\omega)$. This is evaluated with the full electron-electron interaction given in Eq. (3.4). Hence the one-particle Green function can be written as

$$G^0_\nu(\omega)=\frac{1}{\omega-\epsilon^0_\nu} \ ,$$

and

$$G_\nu(\omega)=G^0_\nu/[1-\bar{\Sigma}_\nu(\omega)G^0_\nu(\omega)] \tag{3.5}$$

with

$$\bar{\Sigma}_\nu(\omega)=\Sigma_\nu-\langle\phi_\nu|V_c(r,n(r))|\phi_\nu\rangle \ .$$

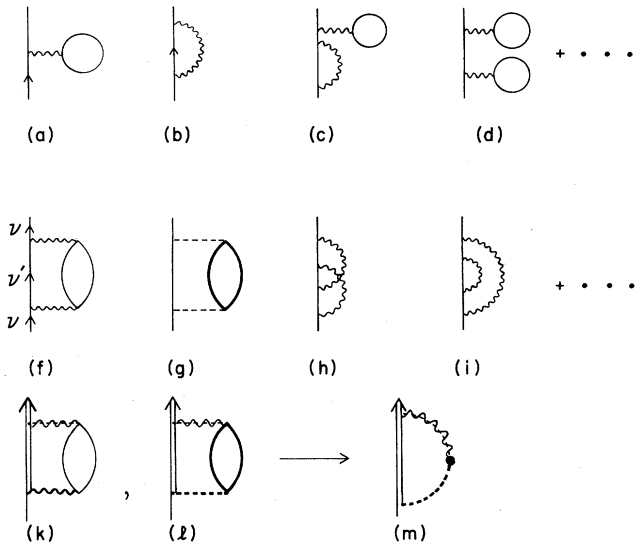

FIG. 2. The contributions to the electron self-energy. Wavy line: electron-electron interaction; dashed line: electron-ion interaction; thin lines: electron propagator G^0; thick lines: ion propagators. Diagrams (a)—(d) are Hartree-Fock-type diagrams arising from the electron subsystem. These and the corresponding Hartree terms from the ions are already included in the DFT calculation. Second-order diagrams (f)—(i). The DFT correlation potential V_c is used in static models to mimic the contribution from the screened form of (f). In the dynamic correlation model CIP, (f) and (g) are replaced by (k) and (l). The ion-density fluctuation loop in (l) is further reduced to (m) by a static approximation. (k), (l), and (m) contain the renormalized propagator and the screened interactions.

This substraction procedure makes the results of the calculation somewhat independent of the form of the exchange correlation used in the DFT calculation.

Since the Hartree-Fock-type terms have been already included in ϵ_ν^0, the leading-order contributions to $\Sigma_\nu(\omega)$ are from the second-order diagrams shown in Figs. 2(f)–2(i). The contributions from diagrams other than 2(f) and 2(g) are assumed to be small except close to zero temperature and hence will be neglected in this study. Hence we write, in second order

$$\Sigma_\nu^{(2)}(\omega)=\Sigma_{\nu,ee}^{(2)}+\Sigma_{\nu,ei}^{(2)} , \tag{3.6}$$

where the two terms correspond to Figs. 2(f) and 2(g). In Ref. 5 it was shown how these second-order terms [Eq. (3.14) of Ref. 5 is essentially the same as Eq. (3.11) of this paper] could be calculated from the Heisenberg equations of motion of the retarded anticommutator propagator $G_\nu(\omega+ie)=\langle\langle a_\nu, a_\nu^\dagger\rangle\rangle$. Alternatively, $\Sigma_\nu^{(2)}(\omega)$ can be calculated by straightforward use of the rules of diagrammatic perturbation theory at finite temperatures,[11] or those of multiple-scattering techniques, coherent-potential approximations, etc., used in the theory of disordered materials.[12,13] The result can be extended to include summations of polarization loops to give the forms inclusive of screening. This is denoted by the tilde on $\tilde{V}_{ie}$ and $\tilde{V}_{ee}$. Thus

$$\Sigma_{\nu,ee}(\omega)=\sum_{\vec{q},\nu',\nu_1,\nu_2}\frac{|\langle\nu\nu_1|\tilde{V}_{ee}(q)\nu_2\nu'\rangle|^2[\langle a_1^\dagger a_2 a_2^\dagger a_1\rangle-\bar{n}_\nu(\bar{n}_1-\bar{n}_2)]}{\omega-\epsilon_\nu^0+\epsilon_1^0-\epsilon_2^0} , \tag{3.7a}$$

$$\Sigma_{\nu,ei}(\omega)=\sum_{\vec{q},\nu',k}\frac{|\langle\nu|\tilde{V}_{ie}(q)|\nu'\rangle|^2[\langle b_{\vec{k}}^\dagger b_{\vec{k}+\vec{q}}\rho_q^\dagger\rangle-\bar{n}_\nu(\bar{\rho}_{\vec{k}}-\tilde{\rho}_{\vec{k}+\vec{q}})]}{\omega-\epsilon_\nu^0+E_{\vec{k}}-E_{\vec{k}+\vec{q}}} . \tag{3.7b}$$

Here ν_1 and ν_2 have been replaced by 1 and 2 for brevity.

The screening of the potential has to be introduced so as to avoid double counting of diagrams and the forms used will be discussed later. In (3.7b) $\bar{\rho}_{\vec{k}}=\langle b_{\vec{k}}^\dagger b_{\vec{k}}\rangle$ is the number of ions having the kinetic energy $E_{\vec{k}}=k^2/2M$, the ion mass being M.

Equations (3.7) contain the unrenormalized energies ϵ_ν^0, ϵ_1^0, and ϵ_2^0. However, it is known from similar work in related fields that renormalization of at least the internal propagator $G_\nu(\omega)$ is necessary, as indicated by the double line for G_ν in Figs. 2(k) and 2(l). Hence we rewrite the denominators of (3.7) as

$$\begin{aligned}&\omega-[\epsilon_\nu^0+\Sigma_\nu(\omega)]+\epsilon_{\nu_1}^0-\epsilon_{\nu_2}^0 ,\\ &\omega-[\epsilon_\nu^0+\Sigma_\nu(\omega)]+E_{\vec{k}}-E_{\vec{k}+\vec{q}} .\end{aligned} \tag{3.8}$$

The renormalization of the energy difference $\epsilon_{\nu_1}^0-\epsilon_{\nu_2}^0$ is not considered in view of further approximations which will be carried out (see below) in order to obtain a numerically tractable form of the polarization loops. The renormalization of the denominator now introduces the added numerical problem that Σ_ν has to be determined self-consistently.

Once the self-energy is determined the level population can be calculated from the spectral function via

$$2f_\nu=-\frac{2}{\pi}\int_{-\infty}^{+\infty}\frac{\mathrm{Im}G_\nu(\omega)}{1+e^{\omega/T}}d\omega . \tag{3.9}$$

For infinitely sharp lines $\mathrm{Im}G_\nu(\omega)$ reduces to a δ function and (3.9) gives the usual Fermi distribution. If the level-shape function $\mathrm{Im}G_\nu(\omega)$ could be characterized by a width γ defining a Lorentzian profile, Eq. (3.9) may be easily evaluated without having to calculate $G_\gamma(\omega)$ for a large number of values of ω.

A. Tractable form of the self-energy

Let us first consider the second-order ion-density fluctuation contribution $\Sigma_{\nu,ei}^{(2)}(\omega)$. We shall first of all assume that the dynamic ion-polarization effects can be neglected as shown by the static approximation of Figs. 2(l) and 2(m). Here the ion-polarization loop is replaced by a point. Equation (3.8) is replaced by

$$\Sigma_{\nu,ei}^{(2)}(\omega)=\sum_{q,\nu'}\frac{|\langle\nu|\tilde{V}_{ie}(q)|\nu'\rangle|^2\langle\rho_q\rho_q^*\rangle_{\mathrm{static}}}{\omega-\epsilon_\nu^0-\Sigma_\nu^{(2)}(\epsilon_\nu^0)} , \tag{3.10}$$

where

$$\langle\rho_q\rho_q^*\rangle_{\mathrm{static}}=\bar{\rho}S(q)$$

is the static structure factor of the ion subsystem. This is related to the ion-pair distribution function $g_{ii}(r)$ by

$$S(q)=1+\bar{\rho}\int[g_{ii}(r)-1]e^{i\vec{q}\cdot\vec{r}}d\vec{r}$$

and hence is known from the DFT calculation. Note that Eq. (3.10) is equivalent to the self-energy expression used in the theory of disordered materials[12] and liquid metals.[14]

Let us now consider the more complicated problem of evaluating the electron contribution to the self-energy given by (3.7). In the case of electron density fluctuations we are not entitled to make a static approximation of the sort made for the ions. Owing to the high velocity of the electrons coupled with their quantum nature we need to evaluate the quantities dynamically.

To begin with we replace $\langle a_1^\dagger a_2 a_2^\dagger a_1\rangle$ by its Hartree-Fock form:

$$\begin{aligned}\langle a_1^\dagger a_2 a_2^\dagger a_1\rangle&\rightarrow\langle a_1^\dagger a_1(1-a_2^\dagger a_2)\rangle\\&=\bar{n}_{\nu_1}(1-\bar{n}_{\nu_2}) .\end{aligned}$$

Then, neglecting screening for the moment, the second-order form of Eq. (3.7) becomes

$$\Sigma^{(2)}_{\nu,ee}(\omega)=\sum_{\vec{q},\nu'} V_q^2 \,|\langle \nu | e^{i\vec{q}\cdot\vec{r}} | \nu' \rangle|^2 \sum_{1,2} \frac{|\langle \nu_1 | e^{-i\vec{q}\cdot\vec{r}} | \nu_2 \rangle|^2 [\bar{n}_1(1-\bar{n}_2)-\bar{n}_{\nu'}(\bar{n}_1-\bar{n}_2)]}{\tilde{\omega}_{\nu'}+\epsilon^0_1-\epsilon^0_2} \tag{3.11}$$

where $\tilde{\omega}_{\nu'}=\omega-\epsilon^0_{\nu'}-\Sigma^{(2)}_{\nu'}(\epsilon^0_{\nu'})$.

Now we assume that the complete basis set $\{\phi_\nu\}$ can be replaced by the complete set of plane-wave states, at least as far as the evaluation of the polarization insertion is concerned. This is justifiable since the major contribution to the polarizability arises from the positive energy electron states. Then Eq. (3.11) becomes

$$\Sigma^{(2)}_{\nu,ee}(\omega)=\sum_{\vec{q},\nu'} V_q^2 \,|\langle \nu | e^{i\vec{q}\cdot\vec{r}} | \nu' \rangle|^2 \times \sum_{\vec{k}} \frac{\bar{n}_k(1-n_{\vec{k}+\vec{q}})-\bar{n}_{\nu'}(\bar{n}_k-\bar{n}_{\vec{k}+\vec{q}})}{\tilde{\omega}_{\nu'}+\epsilon_{\vec{k}}-\epsilon_{\vec{k}+\vec{q}}} . \tag{3.12}$$

The $\vec{k}$ integration in (3.12) can now be carried out analytically to give the result

$$\Sigma^{(2)}_{\nu,ee}(\omega)=\sum_{\vec{q},\nu'} V_q^2 \,|\langle \nu | e^{i\vec{q}\cdot\vec{r}} | \nu' \rangle|^2 \times [(1-\bar{n}_{\nu'})L^{(1)}_q(\tilde{\omega}_{\nu'})-\bar{n}_{\nu'}L^{(2)}_q(\tilde{\omega}_{\nu'})] , \tag{3.13}$$

where

$$L^{(1)}_{\vec{q}}(\omega)=\sum_{\vec{k}} \frac{\bar{n}_{\vec{k}}(1-\bar{n}_{\vec{k}+\vec{q}})}{\omega+\epsilon^0_{\vec{k}}-\epsilon^0_{\vec{k}+\vec{q}}} , \tag{3.14}$$

$$L^{(2)}_{\vec{q}}(\omega)=\sum_{\vec{k}} \frac{\bar{n}_{\vec{k}+\vec{q}}(1-\bar{n}_{\vec{k}})}{\omega+\epsilon^0_{\vec{k}}-\epsilon^0_{\vec{k}+\vec{q}}} . \tag{3.15}$$

Note that

$$L_{\vec{q}}(\omega)=L^{(1)}_{\vec{q}}(\omega)-L^{(2)}_{\vec{q}}(\omega)$$

is the Lindhard function at finite temperatures.[15] Their classical limits can be expressed in terms of the Dawson function as in Ref. 6. It is interesting to note that the positive and negative frequency components of the Lindhard function couple to the hole (i.e., $1-\bar{n}_{\nu'}$) and particle (i.e., $\bar{n}_{\nu'}$) densities of the fluctuating state ν'.

Further simplification of (3.10) and (3.13) depends on developing numerically convenient representations for the matrix elements and for the Lindhard functions. This is carried out in the Appendix.

B. Approximation to the screened potential

Equations (3.7) and (3.10) contain the screened interactions $\tilde{V}_{ee}(q)$ and $\tilde{V}_{ie}(q)$ which have yet to be specified. The unscreened form of the matrix element in (3.7) can be written as

$$\langle \nu\nu_1 | V_{ee} | \nu_2\nu' \rangle = V_q \langle \nu | e^{i\vec{q}\cdot\vec{r}} | \nu' \rangle \langle \nu_1 | e^{-i\vec{q}\cdot\vec{r}} | \nu_2 \rangle ,$$

where V_q is the bare Coulomb potential. For a one-component plasma, (OCP, electron-gas) it is easy to show that the screened form in the context of Eq. (3.7) is

$$\langle \nu\nu_1 | \tilde{V}_{ee} | \nu_2\nu' \rangle_{\rm OCP} = V_q \frac{\langle \nu | e^{i\vec{q}\cdot\vec{r}} | \nu' \rangle \langle \nu_1 | e^{-i\vec{q}\cdot\vec{r}} | \nu_2 \rangle}{\epsilon(q,\omega-\epsilon^0_{\nu'})} , \tag{3.16}$$

where $\epsilon(q,\omega)$ is the dynamic screening function. In the two-component case we can include the effect of the ion background (taken in the static approximation) by replacing V_q by $\tilde{V}_q$, thus

$$\tilde{V}_q=\frac{4\pi}{q^2+\lambda_i^2} , \tag{3.17}$$

where the volume factor has been suppressed and λ_i is the static screening vector for the ions. Under the conditions studied here λ_i is well approximated by the Debye-Hückel value. We will approximate the electron screening also by a static approximation and write

$$|\langle \nu\nu_1 | \tilde{V}_{ee} | \nu_2\nu' \rangle|^2 = \tilde{V}^i_q \tilde{V}^t_q \,|\langle \nu | e^{i\vec{q}\cdot\vec{r}} | \nu' \rangle \langle \nu_1 | e^{-i\vec{q}\cdot\vec{r}} | \nu_2 \rangle|^2 , \tag{3.18}$$

where $\tilde{V}^i_q$ is given by (3.17) and $\tilde{V}^t_q$ is given by

$$\tilde{V}^t_q=\frac{4\pi}{q^2+\lambda_t^2} . \tag{3.19}$$

Here λ_t^2 is the total screening factor due to electrons and ions. This is determined by fitting to the pair distribution obtained from the DFT calculation. Note that these equations ensure that electron-polarization loops are not double counted [see Figs. 2(k)–2(m)].

The screened ion-electron matrix element appearing in (3.8) can be written (within the same type of static approximation) as

$$|\langle \nu | \tilde{V}_{ie}(q) | \nu' \rangle|^2 = \tilde{V}^e_q \tilde{V}^t_q \,|\langle \nu | e^{i\vec{q}\cdot\vec{r}} | \nu' \rangle|^2 , \tag{3.20}$$

where

$$\tilde{V}^e_q=\frac{4\pi}{q^2+\lambda_e^2}$$

contains the effective electron screening factor, while $\tilde{V}^t_q$ is defined as in (3.19).

The use of static screening in these expressions is somewhat of a limitation which can, however, be largely justified for the type of temperatures and densities used here, within the representation for the finite-temperature Lindhard-type functions used in these calculations (see the Appendix).

Note that the kind of "dielectric catastrophe" envisaged[16] in the metal-insulator transition does not occur in the plasma since the onset of localization does not affect the large majority of the electrons in extended states. Hence no special Lorentz-type corrections are necessary in the screening factors.

Thus the screened forms of the equations used for computing the self-energy are

$$\Sigma_\nu^{ee}(\omega)=\sum_{\vec{q},\nu'}\frac{4\pi}{q^2+\lambda_i^2}\frac{4\pi}{q^2+\lambda_t^2}|\langle\nu|e^{i\vec{q}\cdot\vec{r}}|\nu'\rangle|^2[L_{\vec{q}}^{(1)}(\tilde{\omega})-\bar{n}_{\nu'}L_{\vec{q}}(\tilde{\omega})]\,, \tag{3.21}$$

$$\Sigma_\nu^{ei}(\omega)=\sum_{\vec{q},\nu'}\frac{4\pi\bar{Z}}{q^2+\lambda_e^2}\frac{4\pi\bar{Z}}{q^2+\lambda_t^2}\frac{|\langle\nu|e^{i\vec{q}\cdot\vec{r}}|\nu'\rangle|^2\bar{\rho}S(q)}{\omega-\epsilon_{\nu'}^0-\Sigma_{\nu'}(\epsilon_{\nu'}^0)}\,, \tag{3.22}$$

with $\tilde{\omega}=\omega-\epsilon_{\nu'}\simeq\omega-\epsilon_{\nu'}^0$. The summation over the intermediate state index ν' runs over all bound states (n,l,m) and over the continuum (k,l,m) states (see the Appendix).

IV. DISCUSSION OF THE RESULTS FOR HYDROGEN PLASMA MODELS

In this section we shall discuss the results for the onset of the 1s-symmetry bound state as a function of temperature (T) and density (r_s) for four models of a hydrogen plasma. These are (i) the finite-temperature jellium model where the ion distribution surrounding the central ion is replaced by a rigid uniform neutralizing background,[17] (ii) the fully-ionized-plasma (FIP) model where the effective charge of the field ions $\bar{Z}$ is assumed to be the nuclear charge Z, (iii) the mean-atomic-plasma (MIP) model where $\bar{Z}=(\bar{R}/r_s^e)^3$, as defined by Eqs. (2.12)–(2.15) (this model reduces to the ionic model in the strong coupling limit and gives the isolated atom model in the weak coupling limit), and (iv) generalization of the mean-ion-plasma model to include dynamic correlations in the electron and ion subsystems. This will be called the correlated-ion-plasma (CIP) model. Here $\bar{Z}$ is defined as in MIP and is the model suitable for the calculation of one-electron energies, level shifts, and level widths of electron states in plasmas.

The problem of the onset of localization in a plasma is more usually approached from the atomic limit where it is posed as the problem of temperature and pressure ionization of an atomic electron.[18,19] In the simplest approach, via the Saha equation, the interactions are neglected or estimated by elementary theories which provide prescriptions for avoiding divergencies. The partition function of an atom diverges unless its extent (i.e., for example, the range of its potential) is limited by introducing a characteristic length (or a maximum quantum number) which effectively defines a screened potential. The equilibrium constant K of the Saha equation for the degree of ionization can be calculated from the partition function. At least in the simple theories, K is zero until the onset of localization when it jumps discontinuously to a finite value. Note that in the more detailed treatment given here the localization proceeds though intermediate stages where the electron tunnels (hops) over many centers (Fig. 1) and hence there would be no discontinuous parameter.

Returning to the simple static screened potential

$$V(r)=e^{-\lambda r}/r\,, \tag{4.1}$$

where $\lambda=3\alpha/\sqrt{r_s}$ a.u., $\alpha=[4/(9\pi)]^{1/3}$ in Thomas-Fermi theory ($T=0$) and $\lambda=(3/Tr_s^3)^{1/2}$ in Debye-Hückel theory, at least one bound state exists unless[20,21]

$$\lambda\gtrsim 1\,. \tag{4.2}$$

Much of the early work on plasma ionization of bound states started off from this property of the Coulomb field. The early work on the Mott transition also used (4.1) and Mott gave the condition[7]

$$r_s\gtrsim 1.55 \quad \text{at } T=0 \tag{4.3}$$

for the onset of extended states in a crystalline lattice of hydrogen atoms. More recent discussions[22] are usually based on the Hubbard model[23] and show that even the short-range part of the Coulomb interaction is sufficient to produce localization. Attempts have been made to describe plasmas[24] and liquid metals[25] using a Hubbard model for the electron subsystem and a lattice gas model for the ion subsystem. Such models are too crude to afford a realistic description of plasma processes but could be useful in some limiting situations. In addition to the above screening transition (or Mott transition), localization can also be produced through lack of long-range order[8] (in the ion subsystem). This effect is usually discussed in terms of the Anderson transition. In a plasma, the finite probability of finding other ions inside a mean ionic radius $\bar{R}$ in MIP takes account of "positional" disorder.

In view of the above discussion we may note that (i) the jellium models are limited to Mott-type localization generated by electron-screening and (ii) models which contain a responding ion-distribution incorporate localization arising from screening and some Anderson-type mechanisms. Finally, the introduction of dynamic density fluctuation effects via self-energy corrections enables one to transcend the one-electron DFT-type limitations in the analysis. The existence of finite damping implies that there is no such thing as complete localization.

A. Jellium model

In the jellium model the DFT equations are solved self-consistently for a single proton and a responding system of electrons, but with the field ions replaced by a uniform nonresponding background which ensures charge neutrality. The potential $V_e(r)$ felt by an electron involves $-Z/r, -V_p(r), V_{\rm xc}^e(r)$ as in (2.9), and depends on the density and temperature (r_s^e and T).

In Debye-Hückel type models the screening parameter attempts to account for the effect of r_s^e and T simultaneously. The replacement of $V_e(r)$ by the Debye-Hückel model may be valid in the classical limit, $(T/E_F)\gg 1$, but would be far less satisfactory than the finite-temperature Thomas-Fermi or Hartree-Fock models.[26] These latter models depend on r_s^e and T separately and their predictions would lie between the Debye-Hückel model and the DFT model.

Results for ϵ_{1s} obtained for the finite-temperature DFT-jellium model are shown in Fig. 3 (see also Table II). We have also shown, in two cases ($r_s=1, r_s=4$), the curves corresponding to the Debye-Hückel potential.

B. Two-component plasma models

Here we consider the fully-ionized-plasma (FIP) model, where the field-ions are assumed to be fully ionized, i.e., $Z=\bar{Z}$, and the mean-ion-plasma model, $\bar{Z}=(\bar{R}/r_s^e)^3$. The latter reduces to the FIP model in the high-density, low-T limit and to the isolated atom case for the weak coupling limit.

DFT results for ϵ_{1s} obtained for the FIP model, $\bar{Z}=Z$ are given in Table II and displayed in Fig. 4. In Fig. 4 we have also displayed the DFT results from the MIP model for the cases $r_s=1$, 2, and 3. It is seen that MIP lies close to the FIP model for, say, $r_s=1$ (high density), while it moves away from the FIP model for $r_s=3$. We believe that the MIP provides a correct, consistent model for defining an atom immersed in a plasma. The eigenvalues ϵ_{1s} for the MIP model are given in Table II.

C. Correlated-ion-plasma model

The mean-ion-plasma model is still a DFT model and hence the single-particle energy levels and level properties have to be calculated from the one-particle Green function, as in Eqs. (3.5)—(3.8). The self-energy calculation generates the shifted and broadened single-particle levels and the level populations in a scheme equivalent to a self-consistent treatment of density-fluctuation correlations by time-dependent perturbation theory on the screened interaction potentials. The actual calculations for this correlated-ion-plasma (CIP) model were carried out using Eqs. (3.21) and (3.22) together with the representations for the Lindhard-type functions and the matrix elements given in the Appendix.

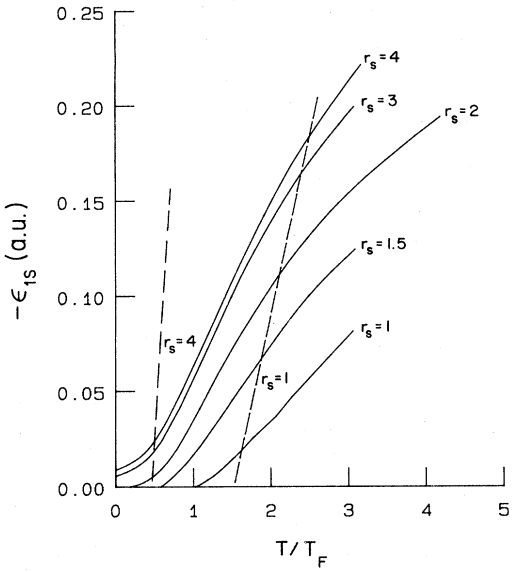

FIG. 3. The 1s symmetry eigenvalue ϵ_{1s} (a.u.) in the jellium model. Results for $r_s=1$ and 4 for the Debye-static screened model are also given as dashed lines.

Table II provides a comparison of the 1s energy predicted by the four models. The jellium model, FIP, and MIP provide no information on level widths, unlike CIP. In CIP the level populations are calculated from Eq. (3.9) using the width γ evaluated from ImΣ, assuming a Lorentzian level profile.

Comparison of the results for $r_s=3$ for the different

TABLE II. Comparison of the results of the 1s state obtained by four models of the hydrogen plasma (see Sec. IV). The energies ϵ_{1s} are in atomic units. μ_c is the correlation part of the exchange-correlation potential V_{xc} used in the DFT calculation. $2f_{1s}$ is the level population for the 1s level which spreads over many ion centers (see Fig. 1). In the CIP model dynamic correlations are included and the level energy ϵ_{1s}, level width γ_{1s}, and the level population are calculated from the one-particle Green function (see Table III).

			Jellium model		FIP model		MIP model		CIP model		
r_s	T/E_F	$-\mu_c^{DFT}$	ϵ_{1s}^{DFT}	f_{1s}^{DFT}	ϵ_{1s}^{DFT}	f_{1s}^{DFT}	ϵ_{1s}^{DFT}	f_{1s}^{DFT}	ϵ_{1s}	$100\times\gamma_{1s}$	f_{1s}
3	0.5	0.0625	−0.019	0.8414	−0.0092	0.8288	−0.0196	0.8427	+0.0275	20.29	0.5615
	1.0	0.0917	−0.059	0.5660	−0.0365	0.5392	−0.0528	0.5589	−0.0045	3.80	0.4917
	1.5	0.1299	−0.102	0.3973	−0.0690	0.3720	−0.0858	0.3848	−0.0350	1.05	0.3474
	2.0	0.1363	−0.140	0.2913	−0.0986	0.2710	−0.1134	0.2782	−0.0606	0.39	0.2537
	3.0	0.1374	−0.196	0.1734	−0.1440	0.1615	−0.1545	0.1639	−0.1066	0.09	0.1536
	4.0	0.1329			−0.1751	0.1075	−0.1829	0.1084	−0.1458	0.03	0.1042
2	1.0	0.1469	−0.037	0.5146	−0.0059	0.4978	−0.0124	0.5014	+0.0422	5.23	0.4683
	1.5	0.1693	−0.073	0.3445	−0.0258	0.3293	−0.0348	0.3321	−0.0141	2.10	0.3266
	2.0	0.1779	−0.105	0.2466	−0.0476	0.2352	−0.0567	0.2370	−0.1008	0.67	0.2465
	3.0	0.1785	−0.154	0.1455	−0.0853	0.1395	−0.0938	0.1401	−0.2089	0.16	0.1509
	4.0	0.1714	−0.189	0.0973	−0.1149	0.0938	−0.1208	0.0941	−0.2591	0.05	0.1007
1	2.0	0.2792	−0.036	0.2278	+0.0000	0.2260	−0.0000	0.2260	−0.4571	0.61	0.2486
	2.5	0.2814			−0.0038	0.1692	−0.0043	0.1692	−0.5522	0.31	0.1872
	3.0	0.2830	−0.080	0.1338	−0.0122	0.0889	−0.0131	0.1324	−0.6265	0.17	0.1459

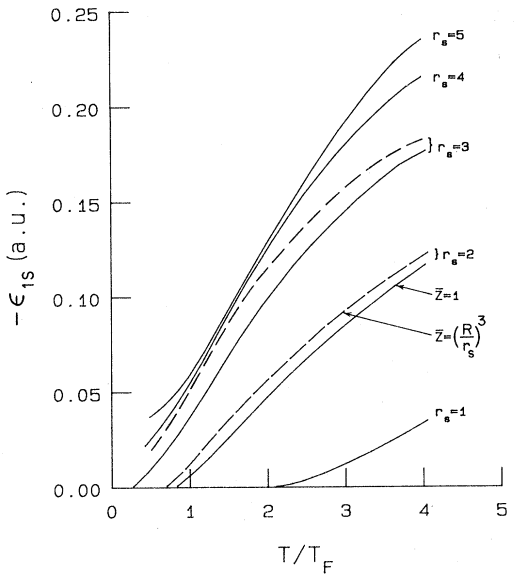

FIG. 4. The $1s$ symmetry eigenvalue ϵ_{1s} for the FIP ($\bar{Z}=1$, solid curves) and MIP ($\bar{Z}=R^3/r_s^3$, dashed curves) models (see Table II). For $r_s=1$ the curves for FIP and MIP are indistinguishable. MIP for $r_s=4$ and 5 are not shown.

models shows that the introduction of a responding ion profile weakens the bound state. Thus ϵ_{1s} is shifted upwards (red shift) so that $\epsilon_{1s}^{\text{jell}}<\epsilon_{1s}^{\text{MIP}}<\epsilon_{1s}^{\text{FIP}}<\epsilon_{1s}^{\text{CIP}}$. The destabilization arising from the dynamic correlations is sufficiently strong to destroy the weak $1s$ levels at $r_s=3, T/T_F=0.5$ and $r_s=2, T/T_F=1.0$ predicted by the static models. However, at higher temperatures ($T\gtrsim 2, r_s=2$) and densities the dynamic correlations are found to deepen the level, giving a blue-level shift. From Table III we see that both Σ^{ee} and Σ^{ei} make significant contributions to the level shift.

The high-density ($r_s=1$) data presented in Tables II and III also imply a strong stabilization (i.e., deepening) of the level due to correlation effects as the temperature increases. The trend in the value of the static correlation potential μ_c of DFT is also in keeping with this. However, from Table III we see that the electron-ion contribution Σ^{ei} has become suspiciously large. This has at least two implications, (i) the DFT calculation for such systems should have not only $V_{\text{xc}}^e, V_{ii}^c$, but also the electron-ion correlation potential V_{ei}^c, (ii) the approximations made in arriving at Eq. (3.22) for $\Sigma_\nu^{ei}(\omega)$ have to be reviewed. Thus, for example, a weakly localized electron may be considered as an electron very close to the $k=0$ extended state. For such an electron the motion of the ions may be far from negligible and the use of the static form (3.22) may be invalid. In fact, a calculation Σ_{1s}^{ei} in the high-temperature limit (when the Lindhard functions $L, L^{(1)}$ can be written in terms of the Dawson function) suggests that if

$$|\epsilon_{1s}| \lesssim T$$

then a *dynamical description of ion-electron correlations becomes necessary.* Such a description can be obtained if $\Sigma_\nu^{ei}(\omega)$ is evaluated in a manner parallel to the evaluation of $\Sigma_\nu^{ee}(\omega)$. We believe that this, together with the inclusion of V_{ei}^c in the DFT calculation will reduce $\text{Re}\Sigma_{1s}^{ei}(\omega)$ for $r_s=1$ given in Table III to magnitudes comparable to or less than $\Sigma_{1s}^{ee}(\omega)$. This could still imply a blue shift of the levels for these densities and temperatures.

The level width calculated for $\Sigma_\nu(\omega)$ contains electron-electron and electron-ion contributions. If we examine the electron-ion contribution, Eq. (3.10), we see that if we set $\nu=\vec{k}, \nu'=\vec{k}-\vec{q}$ and ignore the renormalization of the denominator, then

$$\Gamma(\omega,k)=\text{Im}\Sigma_{k,ei}(\omega) = \int |\tilde{V}(q)|^2 S(q)\delta(\omega-\epsilon_{\vec{k}-\vec{q}})d\vec{q}\ . \tag{4.4}$$

TABLE III. Details of the calculation of the self-energy which enters into the one-particle Green function $G_{1s}(\omega)$. Here ϵ_{1s}^0 is the zeroth-order energy provided by the MIP-DFT calculation. Σ^{ee} and Σ^{ei} are the electron-electron and electron-ion contributions to the self-energy, and γ is the level width (atomic units).

r_s	T/T_F	$-\mu_c^{\text{DFT}}$	ϵ_{1s}^0	$\text{Re}\Sigma^{ei}$	$\text{Re}\Sigma^{ee}$	ϵ_{1s}	$\text{Im}\Sigma^{ei}\times 100$	$\text{Im}\Sigma^{ee}\times 100$	$\gamma\times 100$
3	0.5	0.0625	−0.0196	−0.0034	−0.0119	+0.0275	−0.290	−20.00	20.29
	1.0	0.0917	−0.0528	−0.0115	−0.0319	−0.0045	−0.310	−3.49	3.80
	1.5	0.1299	−0.0858	−0.0223	−0.0419	−0.0350	−0.130	−0.92	1.05
	2.0	0.1363	−0.1134	−0.0331	−0.0471	−0.0606	−0.053	−0.33	0.39
	3.0	0.1374	−0.1545	−0.0514	−0.0524	−0.1066	−0.014	−0.077	0.09
	4.0	0.1329	−0.1829	−0.0630	−0.0544	−0.1458	−0.005	−0.027	0.03
2	1.0	0.1469	−0.0124	−0.0545	−0.0378	+0.0422	−2.290	−2.93	5.23
	1.5	0.1693	−0.0348	−0.0836	−0.0649	−0.0141	−1.120	−0.98	2.10
	2.0	0.1779	−0.0567	−0.1246	−0.0975	−0.1008	−0.230	−0.44	0.67
	3.0	0.1785	−0.0928	−0.1718	−0.1228	−0.2089	−0.052	−0.11	0.16
	4.0	0.1714	−0.1208	−0.1856	−0.1241	−0.2591	−0.016	−0.036	0.05
1	2.0	0.2792	−0.0000	−0.5009	−0.2354	−0.4571	−0.300	−0.31	0.61
	2.5	0.2814	−0.0043	−0.5495	−0.2799	−0.5522	−0.150	−0.16	0.31
	3.0	0.2830	−0.0131	−0.5866	−0.3099	−0.6265	−0.083	−0.089	0.17

This is just a measure of the scattering of electrons by the screened ion centers in the Born approximation. If $I(\theta)$ is the scattering cross section due to a single ion, the Bhatia-Krishnan[27]-Ziman[28] theory shows that the scattering due to two atoms at a distance $\vec{r}$ from each other is given by

$$I(\theta)\,|\,\{1+\exp[i(\vec{k}-\vec{k}')\cdot\vec{r}]\}\,|^2\,. \tag{4.5}$$

Averaging over all r, the scattered intensity becomes $I(\theta)S(q)$ where $q=|\vec{k}-\vec{k}'|=2k\sin(\theta/2)$ and $S(q)$ is the structure factor. If the scattering leads to a mean free path $L=\tau v$ for the electron, where τ is the electron lifetime and v the electron velocity, then the conductivity σ is given by (note $e=\hbar=m=1$)

$$\begin{aligned}&\sigma=\bar{n}\,\tau\,,\\&1/\tau v=2\pi\rho\int_0^{-\pi}I(\theta)(1-\cos\theta)S(q)\sin\theta\,d\theta\,,\end{aligned} \tag{4.6}$$

and $1/\tau$ is just the quantity given by (4.4) which specifies a k-dependent mean life $\tau(k)$.

When ν is a weak bound state the electron is still very far from the atomic limit (see Fig. 1) and hence still suffers scattering from the ion distribution. Thus the contribution to γ in Tables II and III arising from Σ_{ie} may be interpreted as a contribution to the electrical conductivity arising from these weakly localized states. In this sense, the mobility "edge" for these electrons may be defined by requiring $\mathrm{Im}\Sigma_{ie}$ to drop to zero. However, owing to the statistical nature of the ion distribution, it is likely that the concept of a minimum conductivity[7] will not be relevant to plasmas.

ACKNOWLEDGMENTS

One of the authors (M.W.C.D.) wishes to thank Dr. Carl Moser, of the Centre Européan de Calcul Atomique et Moléculaire (CECAM), Orsay, for support and hospitality at CECAM. We also thank François Grimaldi of Centre d'Etudes de Limeil, Commissariat à l'Energie Atomique for many discussions and for his role in initiating this project.

APPENDIX: SOME PRACTICAL ASPECTS OF THE CALCULATIONS

In this appendix we give details on the numerical approximations used in evaluating the self-energy, $\Sigma_\nu(\omega)$.

1. Rational approximation for the real part of the Lindhard functions

These functions are defined in (3.14) and (3.15). In the following, we shall work mainly on $L^{(1)}_{\vec{q}}(\omega)$ since, for a complex frequency $\bar{\omega}=\omega+i\tau$, one has

$$\begin{aligned}L_{\vec{q}}(\bar{\omega})&=L^{(1)}_{\vec{q}}(\bar{\omega})-L^{(2)}_{\vec{q}}(\bar{\omega})\\&=L^{(1)}_{\vec{q}}(\bar{\omega})+L^{(1)}_{\vec{q}}(-\bar{\omega})\,.\end{aligned} \tag{A1}$$

Starting from the definition of $L^{(1)}_{\vec{q}}(\bar{\omega})$, (3.14), using the identity

$$\frac{1}{1+e^a}\frac{e^b}{1+e^b}=\left[\frac{1}{1+e^a}-\frac{1}{1+e^b}\right]\frac{1}{1-e^{a-b}}\,,$$

then replacing $\vec{k}$ by $\vec{k}-\frac{1}{2}\vec{q}$, integrating over $k_\perp$ ($\vec{k}=\vec{k}_{||}+\vec{k}_\perp$ with $\vec{k}_{||}$ parallel to $\vec{q}$), one finds easily

$$\begin{aligned}2\pi^2\beta qL^{(1)}_{\vec{q}}(\bar{\omega})=&\int_{-\infty}^{\infty}dy\frac{1}{1-e^{\beta y}}\frac{1}{\bar{\omega}+y}\\&\times\ln\left[\frac{1+E_+(y,q)}{1+E_-(y,q)}\right],\end{aligned} \tag{A2}$$

$$2\pi^2\beta qL_{\vec{q}}(\bar{\omega})=\int_{-\infty}^{\infty}dy\frac{1}{\bar{\omega}+y}\ln\left[\frac{1+E_+(y,q)}{1+E_-(y,q)}\right], \tag{A3}$$

where

$$E_\pm(y,q)=\exp\left[-\frac{1}{2}\beta\left[\pm\frac{y}{q}+\frac{q}{2}\right]^2+\eta\right],$$

$$\eta=\beta\mu\,.$$

In the numerical applications we have done, the imaginary part of $\bar{\omega}$ is everywhere small, so that one gets immediately

$$\begin{aligned}&2\pi\beta q\,\mathrm{Im}L_{\vec{q}}(\bar{\omega})=-\ln\frac{1+E_+(\omega,q)}{1+E_-(\omega,q)}\,,\\&\mathrm{Im}L^{(1)}_{\vec{q}}(\bar{\omega})=\mathrm{Im}L_{\vec{q}}(\bar{\omega})/(1-e^{-\beta\omega})\,.\end{aligned} \tag{A4}$$

(A4) is exact in the limit $\tau=\mathrm{Im}\bar{\omega}\to 0$.

With the appropriate change of variable, the real part of $L_{\vec{q}}(\bar{\omega})$ is rewritten

$$\begin{aligned}\mathrm{Re}L_{\vec{q}}(\bar{\omega})=&(2\pi^{3/2}\beta q)^{-1}[H(\sqrt{\beta/2}x_+)\\&+H(\sqrt{\beta/2}x_-)]\,,\end{aligned} \tag{A5}$$

$$x_\pm=\pm\frac{\omega}{q}-\frac{q}{2}\,, \tag{A6}$$

$$H(X)=\pi^{-1/2}\int_{-\infty}^{\infty}\ln(1+e^{-t^2+\eta})\frac{1}{X-t}dt\,. \tag{A7}$$

The integral in $H(X)$ is to be taken in principal part. The behavior of H at small and large X can be determined by elementary means, and one finds

$$\begin{aligned}&H(X)\sim(2\pi\beta)^{3/2}\eta\sigma X+\cdots\quad\text{as } X\to 0\\&H(X)\sim\tfrac{1}{2}(2\pi\beta)^{3/2}n\frac{1}{X}\left[1+\frac{\theta}{2}\frac{1}{X^2}+\cdots\right]\quad\text{as } X\to\infty,\end{aligned} \tag{A8}$$

where n is the density of the uniform electron gas,

$$n=\frac{\sqrt{2}}{\pi^2}\beta^{-3/2}I_{1/2}(\eta)$$

and with σ and θ defined in terms of standard Fermi functions by

$$\sigma=\frac{1}{2}\frac{I_{-1/2}(\eta)}{I_{1/2}(\eta)}\ ,$$

$$\theta=\frac{2}{3}\frac{I_{3/2}(\eta)}{I_{1/2}(\eta)}\ .$$

The high-temperature limits of σ and θ are 1, and the low-T limits are $\sigma=3/(2\eta)$ and $\theta=2\eta/5$. Looking for a rational approximation of H, we write

$$\mathrm{Re}L_{\vec{q}}(\bar{\omega})=\sqrt{\beta/2}\frac{n\sigma}{q}[F(\sqrt{\beta/2}x_+)+F(\sqrt{\beta/2}x_-)] \quad \text{(A9)}$$

with

$$F(X)=2X\frac{1+aX^2}{1+(2-\theta a)\sigma X^2+2a\sigma X^4}\ . \quad \text{(A10)}$$

(A10) is compatible with (A8) for any value of the parameter a. Now, for $T\to\infty$, $F(x)$ must be a representation of the Dawson function

$$D(x)=2e^{-x^2}\int_0^x e^{t^2}dt\ .$$

In order to recover the exact high-T limit of the ring contribution to the grand potential of the electron gas Ω_r (see Ref. 11, p. 277), one must have

$$1=\frac{4}{\sqrt{\pi}}\int_0^\infty ye^{-y^2}D(y)dy$$

a condition which determines a when D is replaced by F. The high-T value $a=1.14$ is obtained in that way. The following compares the simple form (A10) at high T ($\sigma=\theta=1$) to the Dawson function:

x	$F(x)$	$D(x)$
0.1	0.201	0.199
0.2	0.403	0.390
0.3	0.604	0.565
0.4	0.791	0.720
0.5	0.947	0.849
0.6	1.054	0.950
0.8	1.114	1.064
1.0	1.034	1.076
1.2	0.910	1.015
1.4	0.791	0.913
1.6	0.691	0.800
1.8	0.610	0.694
2.0	0.544	0.603
2.5	0.426	0.446
5.0	0.204	0.204

The maximum deviation is 14%. (A7) provides results which are much more accurate than any kind of "plasmon-pole"-type approximation. At $T=0$, $\mathrm{Re}L_{\vec{q}}(\omega=0)$ is of the form

$$L_{\vec{q}}(\omega=0)=-\frac{k_F}{\pi^2}\mathscr{L}\left[\frac{q}{2k_F}\right]\ ,$$

where k_F is the Fermi momentum ($2\mu=k_F^2$). This implies that the parameter a must be proportional to η^{-1} at low T. We write

$$a=1.14\left[p\sigma+(1-p)\frac{1}{\theta}\right]\ ,$$

satisfying the high- and low-T limits, and try to optimize p in order to get the best fit of $L_{\vec{q}}(0)$. In fact, the sensitivity to p is small: for instance, at $q=2k_F$, $\pi^2L_{\vec{q}}/k_F$ varies from -0.334 for $p=1$ to -0.355 for $p=0$ (compare with the exact value of -0.500). Finally, for the sake of simplicity, we have chosen $p=1, a=1.14\sigma$ for any temperature. The behavior of the approximate $L_{\vec{q}}(\omega)$ at $T=0$ is physically correct, although the weak logarithmic singularity of the exact function is not reproduced and the accuracy is poorer than for high T.

Now we derive a corresponding approximation for $L^{(1)}_{\vec{q}}(\bar{\omega})$ which, in analogy with (A5)–(A7), can be written

$$\mathrm{Re}L^{(1)}_{\vec{q}}(\bar{\omega})=(2\pi^{3/2}\beta q)^{-1}[\bar{M}(\sqrt{\beta/2}x_+,y)+M^+(\sqrt{\beta/2}x_-,y)]\ , \quad \text{(A11)}$$

$$y=q\sqrt{2\beta}\ , \quad \text{(A12)}$$

$$M^\pm(x,y)=\pi^{-1/2}\int_{-\infty}^{\infty}\ln(1+e^{-t^2+\eta})\frac{1}{x-t}f^\pm(t,y)dt\ , \quad \text{(A13)}$$

$$f^\pm(t,y)=\{1-\exp[\pm(ty+y^2/4)]\}^{-1}\ . \quad \text{(A14)}$$

In (A13) the functions $M^\pm$ differ with respect to function H in (A7) owing to the extra factor $f^\pm(t,y)$. Note that the sum of f^+ and f^- is just unity. A detailed calculation of $M^\pm$ would be very complicated, so we decided to use a crude approximation which consists in neglecting the t dependence of $f^\pm$. Thus (A13) becomes

$$M^\pm(x,y)=f^\pm(y)H(x)$$

and then, with F as an approximate form of H,

$$\mathrm{Re}L^{(1)}_{\vec{q}}(\bar{\omega})=\sqrt{\beta/2}\frac{n\sigma}{p}\{f^-(y)F(\sqrt{\beta/2}x_+)+[1-f^-(y)]F(\sqrt{\beta/2}x_-)\}. \quad \text{(A15)}$$

The most simple form which can be obtained for $f^-(y)$ is a constant (independent of q) which is found from the exact behavior of $L^{(1)}_q(\bar{\omega})$ at $q=0$. This gives

$$f^-(y)=\frac{1+\sigma}{2}\ . \quad \text{(A16)}$$

Better approximations can be found, but (A16) already gives the following properties [within the approximation for $H(x)$]:

(i) Relation (A1) holds, so that (A15) and (A9) are compatible.

(ii) (A15) is exact at high temperature ($f^-=1$).

(iii) The asymptotic form for large q, $L^{(1)}_q(\bar{\omega})=-2n/q^2$ is correct.

This simple approximation (A15) and (A16) has been used in the calculations presented in Tables II and III.

2. Numerical estimate of the matrix elements

The matrix element of a plane wave $e^{\vec{i}\vec{q}\cdot\vec{r}}$ between the $1s$ bound state $|\nu\rangle$ and a free state $|\nu'\rangle$ is needed to compute the self-energy, as defined in (3.10) and (3.13). The full calculation of the matrix element, for any value of $\vec{q}$, in a wide range of free-state energies (and a large number of angular momenta) would be very time consuming. So we have derived the following interpolation procedure.

Assume that the $1s$ bound state is well described by a normalized exponential

$$|\nu\rangle = Ae^{-\alpha r}, \quad A^2 = \frac{\alpha^3}{\pi}$$

and the continuum state by a plane wave orthogonalized to $|\nu\rangle$

$$|\nu'\rangle = |\vec{k}\rangle = \frac{1}{\sqrt{\Omega}}(e^{\vec{i}\vec{k}\cdot\vec{r}} - be^{-\alpha r})$$

with Ω the volume of the system ($\Omega \to \infty$), and b such that $\langle \vec{k} | \nu \rangle = 0$:

$$b = \frac{8\alpha^4}{(k^2+\alpha^2)^2} .$$

(Note that the overlap does not change the normalization for $\Omega \to \infty$ and α finite.) The matrix element is now

$$\langle \nu | e^{\vec{i}\vec{q}\cdot\vec{r}} | \vec{k} \rangle = 8\pi A\alpha \left[\frac{1}{(|\vec{k}+\vec{q}|^2+\alpha^2)^2} - \frac{16\alpha^4}{(k^2+\alpha^2)(q^2+4\alpha^2)^2} \right] . \quad \text{(A17)}$$

With (A17), averaging over the angles on the squared matrix element is straightforward. This analytic formula has been used in the following manner: For a given free-state energy $E = \frac{1}{2}k^2$, we calculated first the average square of the *exact* matrix element for $q = k$ (using the DFT wave functions). Then we determined the value of α *appropriate to that energy* E by fitting (A17) to the numerical result. Finally, we used that α to compute the matrix element for any desired value of $\vec{q}$, and repeated the procedure for every energy in the continuum.

[1] M. W. C. Dharma-wardana and F. Perrot, Phys. Rev. A 26, 2096 (1982) referred to in the text as DP. See also M. W. C. Dharma-wardana, F. Perrot, and G. C. Aers, *ibid.* 28, 344 (1983).

[2] N. D. Mermin, Phys. Rev. 137, A1441 (1965); W. Kohn and L. J. Sham, *ibid.* 140, A1133 (1965).

[3] See R. M. More, Lawrence Livermore Laboratory Report No. UCRL-84115, 1980 (unpublished); F. J. Rogers and H. E. DeWitt, Phys. Rev. A 8, 1061 (1973).

[4] M. W. C. Dharma-wardana and R. Taylor, J. Phys. C 14, 629 (1981); U. Gupta and A. K. Rajagopal, Phys. Rev. A 22, 2792 (1980) [in this work the authors have used the noninteracting chemical potential in evaluating the ring sum, leading to an incorrect result (opposite sign) for the Debye-Hückel pressure]. See Eq. (105) of U. Gupta and A. K. Rajgopal, Phys. Rep. 87, 261 (1982).

[5] M. W. C. Dharma-wardana, F. Grimaldi, A. Lecourt, and J.-L. Pelissier, Phys. Rev. A 21, 379 (1980).

[6] M. W. C. Dharma-wardana, J. Quant. Spectrosc. Radiat. Transfer 27, 315 (1982).

[7] N. F. Mott, *Metal-Insulator Transition* (Taylor and Francis, London, 1974); *Proceedings of the International Conference on Metal-Nonmetal Transition in Disordered Systems, Edinburgh, 1978,* edited by L. R. Friedman and D. P. Tunstil (Scottish Universities Summer School in Physics, St. Andrews, 1978); *Ill-condensed Matter,* edited by R. Balian, R. Maynard, and G. Toulouse (North-Holland, New York, 1979).

[8] P. W. Anderson, Phys. Rev. 109, 1492 (1958); R. Abou-Charca, P. W. Anderson, and D. J. Thouless, J. Phys. C 6, 1734 (1973); L. Fleishman and P. W. Anderson, Phys. Rev. B 21, 2366 (1980). See also Ref. 7.

[9] J. Friedel, Nuovo Cimento, Suppl. 2, 287 (1958); C. Kittel, *Quantum Theory of Solids* (Wiley, New York, 1963), Chap. 18.

[10] See I. J. Feng, W. Zakowicz, and R. H. Pratt, Phys. Rev. A 23, 883 (1981) for a discussion of Thomas-Fermi models and Debye-Hückel interpolation models. See A. I. Larkin, Zh. Eksp. Teor. Fiz. 38, 1896 (1960) [Sov. Phys.—JETP 11, 1363 (1960)] for an approach involving the decomposition of the partition function.

[11] A. K. Fetter and J. D. Walecka, *Quantum Theory of Many Particle Systems* (McGraw-Hill, New York, 1971), Chaps. 7–9.

[12] S. F. Edwards, Proc. R. Soc. London, Ser. A 267, 518 (1962); Philos. Mag. 6, 617 (1961).

[13] R. J. Elliott, J. A. Krumhansl, and P. H. Leath, Rev. Mod. Phys. 46, 465 (1974).

[14] L. E. Ballentine, Adv. Chem. Phys. 31, 263 (1975); Can. J. Phys. 44, 2533 (1966).

[15] M. W. C. Dharma-wardana, Phys. Lett. 81A, 169 (1981).

[16] T. G. Castner, W. K. Lee, G. S. Cieloszyk, and G. L. Salinger, Phys. Rev. Lett. 34, 1627 (1975).

[17] F. Perrot, Phys. Rev. A 25, 489 (1982).

[18] W. Ebeling, W.-D. Kraeft, and D. Kremp, *Theory of Bound States and Ionization Equilibria in Plasmas and Solids,* in (Ergebnisse der Plasmaphysik und der Gaselektronik, Band V (Akademie, Berlin, 1976).

[19] H. Griem, *Spectral Line Broadening by Plasmas* (Academic, New York, 1976).

[20] L. Hulthén and K. V. Laurikainen, Rev. Mod. Phys. 23, 1 (1951).

[21] F. J. Rogers, H. C. Graboske, Jr., and D. J. Harwood, Phys. Rev. A 1, 1577 (1970).

[22] W. F. Brinkman and T. M. Rice, Phys. Rev. B 7, 1508 (1973).

[23] J. Hubbard, Proc. R. Soc. London 281, 401 (1964), and references therein.

[24] G. E. Norman, Zh. Eksp. Teor. Fiz. 60, 1686 (1971) [Sov. Phys.—JETP 33, 912 (1971)].

[25] S. Nam, T. Ogawa, and T. Matsubara, Prog. Theor. Phys. 61, 736 (1976), and references therein.

[26] B. F. Rozsnyai, Phys. Rev. A 5, 1137 (1972); D. A. Liberman, Phys. Rev. B 20, 4981 (1979), J. Davis and M. Blaha, J. Quant. Spectrosc. Radiat. Transfer 27, 307 (1982).

[27] A. B. Bhatia and K. S. Krishnan, Proc. R. Soc. London Ser. A 194, 185 (1948).

[28] J. L. Ziman, Philos. Mag. 6, 1013 (1961).